JOURNAL OF Applied Polymer SCIENCE

Influence of Silica Nanofiller on the Isothermal Crystallization and Melting of Polyurethane Elastomer

Sanja Lučić Blagojević,[1] Zrinka Buhin,[1] Ivona Igrec[2]

[1]Faculty of Chemical Engineering and Technology, University of Zagreb, Zagreb 10000, Croatia

[2]Croatian Meteorological and Hidrological Service, Air Quality Division, Chemical Laboratory, Zagreb 10000, Croatia

Correspondence to: S. L. Blagojević (E-mail: slucic@fkit.hr)

ABSTRACT: In this article, isothermal crystallization kinetic of the linear hydroxyl polyester urethane (PUR), as well as influence of amorphous silica nanofiller, was investigated. With the aim to investigate the influence of filler surface modification on the crystallization process of polyurethane matrix, nonmodified silica, as well as silica modified with methacrylsilane and octylsilane, were used as fillers for PUR composite preparation. The crystallization kinetics depending on temperature of the isothermal crystallization and volume fraction of filler by using differential scanning calorimetry (DSC) were investigated. The measurements at temperatures 7, 12, and 17°C for PUR and composites with 0.5, 1, 2, and 4 vol % of filler were done. Kinetic parameters of the isothermal crystallization n and K were determined according to Avrami model. Melting of the isothermally crystallized samples was also investigated. Results of the research indicate that by increasing the isothermal crystallization temperature, the crystallization rate of the PUR soft phase decreases and that the perfection of the crystallites is improved. By addition of all fillers up to ≈1 vol %, the crystallization rate increases; however, addition of a higher amount of the filler significantly decreases the crystallization rate. It was found that surface modification can significantly affect crystallization rate and that the nucleation efficiency of silica increases in the following order: methacrylsilane-modified silica < nonmodified silica < octylsilane-modified silica.

KEYWORDS: polyurethanes; composites; crystallization; differential scanning calorimetry

Received 25 July 2012; accepted 19 November 2012; published online
DOI: 10.1002/app.38846

INTRODUCTION

Polyurethane (PUR) elastomers play an important role in various fields of applications such as adhesives, optoelectronics, biotechnology, and many others.[1,2] This class of materials exhibits superior properties related to their high hardness for a given modulus, high abrasion resistance, excellent mechanical properties, and biocompatibility. An important factor that enable such wide spread application is the possibility to tailor the structure and properties by varying the type and ratio of starting components during processing. PUR elastomers are block copolymers, consisting of rigid and flexible segments. Because of the difference in polarity, that is, thermodynamical incompatibility, these segments separate into soft and hard phases. The widespread application of the PUR elastomers is the reason for extensive research carried out in the fields of novel type synthesis and structure-properties relationship.[3–5]

Theory of block copolymers, one of whose components is crystallizable, while other component is noncrystallizable and of whose components are incompatible have been studied extensively.[6,7] Compared with other types of polymers, these block copolymers have a unique equilibrium limited lamellar structure. Theory predicts that in this type block copolymers folding of the crystallizable blocks exist at equilibrium due to the thermodynamic forces between the crystalline and amorphous domains. For this reason, they have equilibrium lamellar structure that can be obtained by annealing, usually in the presence of good solvent for the amorphous phase. The equilibrium domain sizes are determined by packing constraints as well as the balance of the total energy of chain folding in the crystalline domains with the associated entropic conformational and stretching free energy of the noncrystallizable blocks in the amorphous domains.

In the last years, polymer-based nanocomposites that contain nanometric size fillers have been extensively studied. The addition of nanofillers instead of the microfillers to polymer material can influence the properties of materials more significantly. The observed phenomena are assigned to the high interfacial polymer/filler area at which the interactions are established. Thus, previous research has shown that by decreasing the particle size of silica fillers a more significant impact on properties of PUR can be achieved.[8–10]

Fumed silica is a synthetic, amorphous material that has spherical particles, which form chain-like, branched aggregates.[11] Depending on the size of primary particles, which is in the range 7–30 nm and can be controlled by synthesis conditions; specific surface area of this type of silica is between 100 and 400 m^2/g. Due to the silanol groups at the surface, silica is hydrophilic, but replacement of silanol groups using different types of silanes changes hydrophilic nature of the filler surface into hydrophobic. Modified silicas that contains dimethylsilyl, trimethylsilyl, octyl, or methacryl groups at the surface are commercially available.[11] To adjust the final application properties, various types of fumed silica are widely used in many industries and important products (paints, coatings, pigments, adhesives, etc.) based on the PUR, epoxy, silicone, polychloroprene, acrylic, etc.[11]

The results of previous investigations showed that the addition of nanosilica improve thermal, rheological, mechanical, and adhesion properties of PURs.[12–18] This enhancement is attributed to the formation of hydrogen bonds between the silanol groups on the nanosilica surface and ester carbonyl groups in PUR soft segments.[12–14] Consequently, the addition of silica to PUR enhances the incompatibility between hard and soft segments thus favoring the phase separation.[16,17]

Our previous investigations of morphology, thermal and mechanical properties of the PUR/silica nanocomposites showed that the addition of silica, as well as its surface modification with methacrylsilane and octylsilane have influence on spherulite morphology and degree of crystallinity and consequently change mechanical properties of PUR.[19]

Many previous investigations[20–26] showed that the particle size, content, and surface characteristics of silica nanoparticles are main factors that affect crystallization behavior of different semicrystalline polymers. Since degree and rate of crystallization affect main properties of semicrystalline polymers, our further aim in this article was to investigate influence of amount and type of silica filler on crystallization kinetics and melting of isothermally crystallized samples. In this work, the isothermal crystallization kinetic of the PUR nanocomposites with nonmodified and methacrylsilane and octylsilane modified silica have been investigated by using the Avrami's model.

EXPERIMENTAL

Materials

For sample preparation predominantly linear hydroxyl polyester PUR elastomer matrix (Desmocoll 620, produced by Bayer, Germany) in form of granules was used. According to producer's specification, Desmocoll 620 is suitable for the formulation of acetone-based adhesives for use on the various materials (leather, rubber, textiles, plastic films, etc). Previous investigation[17] of this PUR matrix prepared from acetone showed that glass transition temperature of soft segments is at −43°C. Desmocoll 620 reaches maximum crystallinity during the slow evaporation of acetone. By heating of Desmocoll 620 prepared from acetone, melting peaks appears with maximum at 45.9°C.

Three different fumed nanosilicas (Table I) manufactured by Degussa, Germany were used as fillers for nanocomposite preparation. According to manufacturer specifications, nominal primary particle size of Aerosil 200 is 12 nm. The modified fillers were obtained by modifying the surface of Aerosil 200 filler with methacrylsilane (Aerosil R711–A711) and octylsilane (Aerosil R805–A805).

Table I. Properties of Fumed Silica

Filler	Surface modification	Specific surface area, S_{BET} (m^2/g)	Tamped density (g/L)
Aerosil 200	-	200	50
Aerosil R 711	Methacrylsilane	150	60
Aerosil R 805	Octylsilane	150	60

Nanocomposite Preparation

The PUR nanocomposite samples were prepared by solvent casting method. A certain amount of PUR granules and filler is mixed with acetone in a defined mass ratio (PUR : acetone = 1 : 5). The mixture was swollen for the next 24 h and then homogenized 3 h on a magnetic stirrer at 250 rpm. Homogenized mixture is left to dry at room temperature in a covered Petri dish to prevent rapid evaporation of acetone, which would cause film porosity. The sample was left to dry until the complete evaporation of acetone. This procedure has been used to prepare sample without fillers and composites with 0.5, 1, 2, and 4 vol % of all three fillers.

Isothermal Crystallization and Melting

Isothermal crystallization behavior and melting of isothermally crystallized PUR and PUR/silica nanocomposites were studied by using a Mettler Toledo 823 differential scanning calorimetry (DSC) instrument. The DSC instrument was calibrated with indium (T_m^0 = 156.4°C and ΔH_f^0 = 28.5 J/g) prior to performing the experiment. For isothermal crystallization experiment, ~ 10 mg of film sample was sealed into an aluminum crucible. The samples were heated to 80°C at a heating rate 10°C/min under a nitrogen atmosphere (50 mL/min), and held 10 min to remove previous thermal history. After that, the samples are cooled very rapidly at a cooling rate 100°C/min to a designed temperature of isothermal crystallization T_c. Our preliminary experiments on PUR matrix in the broader T_c range from −8 to 17°C showed that from −8 to 7°C T_c does not influence on the crystallization rate significantly. The value of t_{max} at isothermal crystallization curve in this range increases slightly. Therefore, influence of silica fillers' amount and surface modification on kinetics of isothermal crystallization was investigated at T_c = 7, 12, and 17°C. At these temperatures, heat flow was recorded in heat flow versus time plot in a period of 45 min. From the enthalpy evolved during crystallization the kinetic of crystallization was evaluated.

To further analyze the structure of the isothermally crystallized sample, immediately after isothermal step at T_c, the sample was further cooled down to −80°C, and after the isothermal stabilization at that temperature in the period of 10 min, samples are heated again till 80°C to record the melting.

RESULTS AND DISCUSSION

Isothermal Crystallization

In our previous work on PUR/silica nanocomposites, it was found that temperatures of melting and crystallization correspond to crystalline soft phase of the PUR matix.[19] Therefore, all crystallization phenomena discussed in the article are related to the crystallization of nonpolar soft segment of the PUR matrix. As examples, the isothermal thermograms of PUR and PUR + A200 0.5 vol % nanocomposites at different temperatures of isothermal crystallizations, T_c, as well as, thermograms of PUR nanocomposites with 1 vol % of different silicas at $T_c = 7°C$ are presented in Figure 1.

The influence of T_c on crystallization is similar for both neat PUR and PUR + silica nanocomposites [Figure 1(a,b)]. Taking into account convex type of crystallization rate versus T_c curves, the obtained results indicate that all experimental crystallization temperatures (7, 12, and 17°C) are higher than the temperature of maximal crystallization rate. The obtained results are in line with the kinetic theory of crystallization according to which as supercooling (the difference between the melting and crystallization temperature) decreases, the crystallization rate gets slower and exothermal crystallization peak becomes broader and flatter. However, for PUR + A200 1% nanocomposites time to reach overall crystallization is shorter than the time for the neat PUR at the same T_c. These results indicate that the addition of nonmodified silica filler increases crystallization rate. Moreover, surface modification of silica nanofiller has also certain influence on crystallization rate [Figure 1(c)]. In comparison to the crystallization behavior of PUR, surface modification of silica filler with methacrylsilane (A711) increases crystallization rate in the similar manner as nonmodified silica (A200), while modification of silica filler with octylsilane (A805) influences on the crystallization of PUR matrix in a different way. At the crystallization curve PUR + A805 1%, it is visible that before main peak another smaller peak appears. The same phenomena but less pronounced can be seen at the curve of the sample with lower amount of this filler (curve PUR + A805 0.5%). The obtained results can be explained as an influence of surface modification of the filler with octylsilane. Namely, as we determined in our previous investigations of these systems[19] modification of the silica filler with octysilane changes polar nature of the nonmodified filler to nonpolar. It can be assumed that the nonpolar A805 filler has a tendency to locate in the nonpolar soft phase of PUR matrix and thus increases the crystallization rate more strongly than nonmodified silica A200. After the first smaller peak at crystallization curve of the sample with A805 filler further process is similar to sample with nonmodified filler.

The isothermal crystallization kinetics of investigated samples at different T_c was analyzed based on Avrami's overall crystallization equation. Based on the assumption that evolution of the released heat and crystallinity are linearly proportional, the relative degree of crystallinity at time t, $X(t)$, can be calculated according to the following equation:

$$X(t) = \frac{\int_0^t (dH_c/dt)dt}{\int_0^{t_\infty} (dH_c/dt)dt} \quad (1)$$

where dH/dt is heat evolution and t_∞ time at crystallization end.

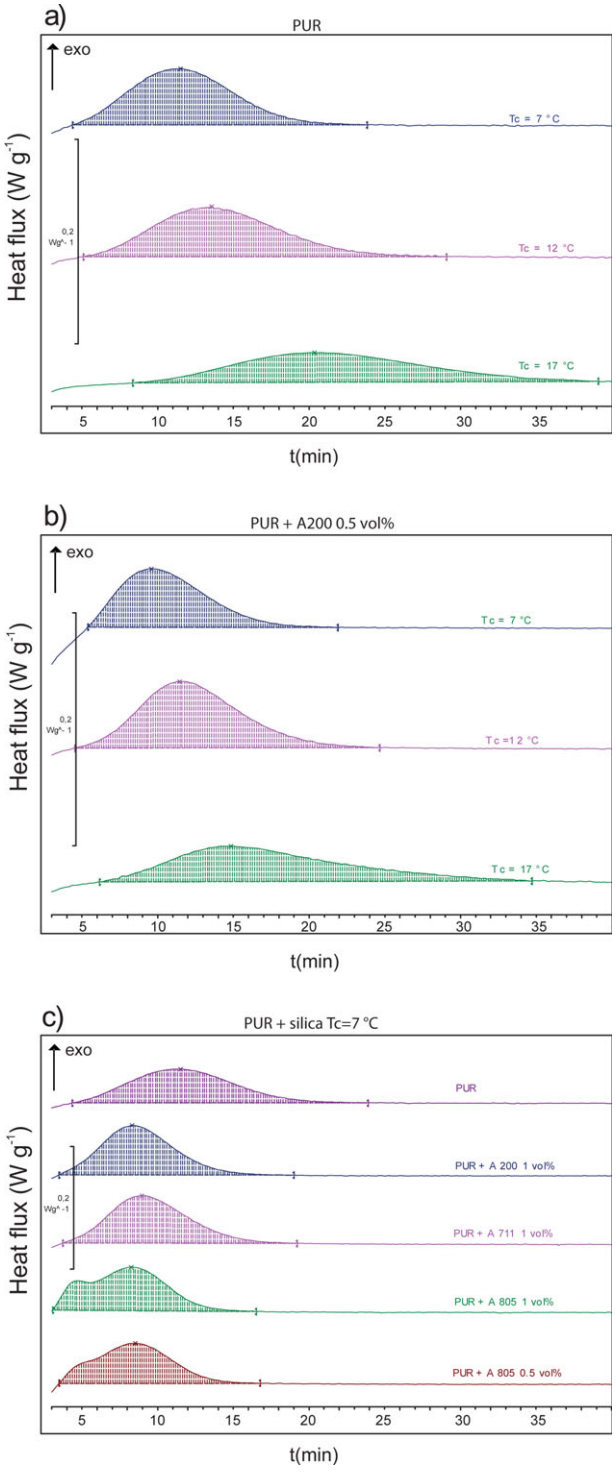

Figure 1. The DSC thermograms obtained during isothermal crystallization for samples (a) neat PUR at different T_c, (b) PUR + A200 0.5 vol % at different T_c and (c) PUR + different types of silica fillers at $T_c = 7°C$. [Color figure can be viewed in the online issue, which is available at wileyonlinelibrary.com.]

In Figure 2, characteristic sigmoidal curves of relative crystallinity versus crystallization time for the same samples as in Figure 1 are presented. It can be seen that for neat PUR [Figure 2(a)] and PUR nanocomposites with nonmodified silica [Figure 2(b)] these curves shift to the right toward higher times with increasing crystallization

Applied Polymer SCIENCE

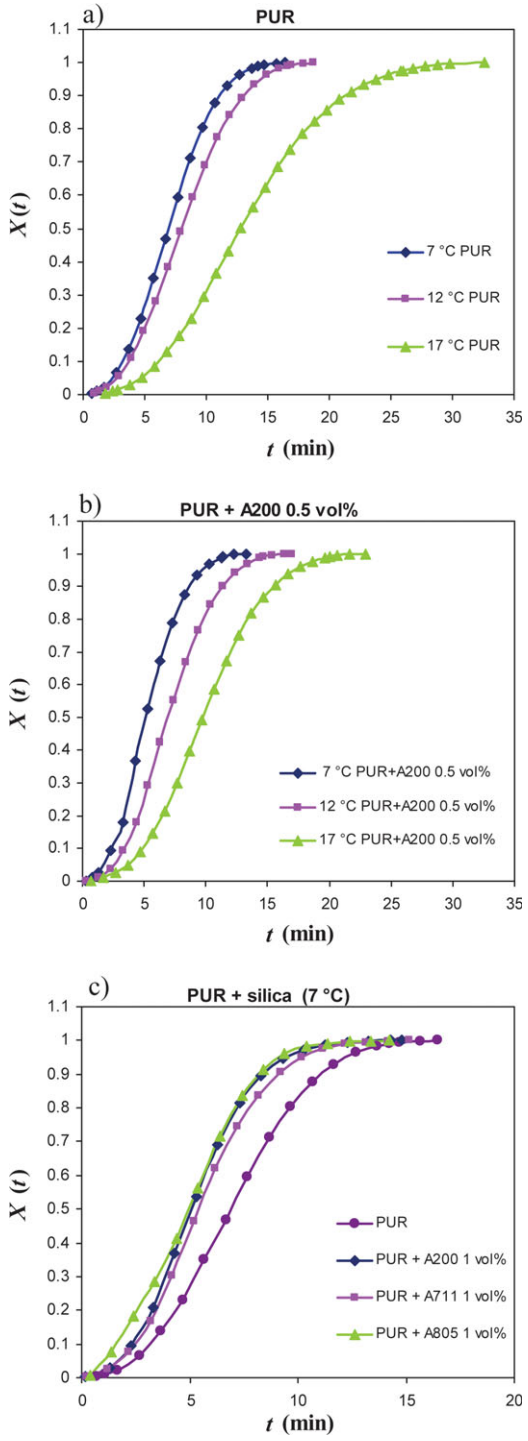

Figure 2. Relative crystallinity $X(t)$ versus crystallization time t for samples (a) neat PUR at different T_c (b) PUR + A200 0.5 vol % at different T_c and (c) PUR + different types of silica fillers at $T_c = 7°C$. [Color figure can be viewed in the online issue, which is available at wileyonlinelibrary.com.]

temperature, thus indicating that crystallization rate becomes slower. From Figure 2(c), it can be observed that modification of silica filler causes some changes in shape and position of this curve.

Avrami model[27,28] is often used to analyze the kinetic of the isothermal crystallization.[26,29–32] According to the Avrami model relative crystallinity, $X(t)$, is related to crystallization time, t, as described by the following equation:

$$X(t) = 1 - \exp(-kt^n) \tag{2}$$

where k is a kinetic constant proportional to nucleation density and to growth rate raised to power n, where n is determined by the dimensionality and nucleation type of the growing semicrystalline spherulites structures.

To obtain values of n and k from fitting experimental data, eq. (2) is used in double logarithmic form as follows:

$$\log\,(-\ln(1 - X(t))) = \log\ k + n\ \log\ t \tag{3}$$

This equation is used to fit experimental data and compare crystallization behavior of neat PUR and PUR nanocomposites at different T_c, as well as to investigate the influence of silica filler surface treatment. Values of n and k determined from the slope and the intersection of the Avrami plots are presented in Table II. Some of the Avrami's plots as examples are presented in Figure 3. For some samples, small deviation from the linearity in the last phase of crystallization that is attributed to the secondary crystallization resulted from spherulite impingement between each other is observed.[21,29] Despite this, values of coefficient of linear regression R^2 presented in Table II, that are very close to 1, confirm that Avrami model can properly describe crystallization of the investigated PUR and PUR/silica nanocomposites, even those with A805 filler that have smaller crystallization peak. The obtained Avrami number n for all investigated samples is in 2.3–2.7 range, thus indicating that spherulites grow in three-dimensional manner.[21]

By using n and k values the crystallization half time, $t_{1/2}$, and time to reach crystallization peak maximum, t_{max}, can be calculated from eqs. (4) and (5), respectively.[26,29,30]

$$t_{1/2} = \left(\frac{\ln 2}{k}\right)^{1/n} \tag{4}$$

$$t_{max} = \left(\frac{n-1}{nk}\right)^{1/n} \tag{5}$$

The values of $(t_{1/2})^{-1}$ and $(t_{max})^{-1}$ are also presented in Table I.

The crystallization rate constant k and $(t_{1/2})^{-1}$, as indicators of crystallization rate for investigated samples, at temperature 7°C are presented in Figure 4(a,b). Differences in curves k and $(t_{1/2})^{-1}$ versus volume fraction of filler for different types of silica filler derive from the fact that crystallization rate constant k [the dimension of which is in $(\text{time})^{-n}$] is function of temperature and also of Avrami exponent n.[26,33,34] Therefore, instead of k the value of K [eq. (6)] that is independent of the Avrami exponent n and has dimension in $(\text{time})^{-1}$ is more preferable constant for crystallization rate.

$$k = K^n \tag{6}$$

Values of K calculated according eq. (6) are presented in Table II and have very similar dependence on fraction of different fillers as values of $(t_{1/2})^{-1}$ presented at Figure 4(b). From the comparison of the crystallization rates for neat PUR and PUR with different concentration of silica, it can be concluded that

Table II. Values for Isothermal Crystallization of Samples

PUR nanocomposite	T_c (°C)	n	$k\ 10^{-3}$, (min^{-n})	R^2	K (min^{-1})	$t_{1/2}^{-1}$ (min^{-1})	t_{max}^{-1} (min^{-1})	ΔH_c, (J/g PUR)
PUR	7	2.45	6.52	0.998	0.159	0.149	0.159	25.45
	12	2.45	4.51	0.998	0.137	0.128	0.137	25.51
	17	2.51	1.11	0.999	0.081	0.077	0.081	25.25
PUR + A200 0.5%	7	2.33	15.38	0.998	0.212	0.195	0.212	24.67
	12	2.58	4.60	0.999	0.150	0.143	0.150	25.23
	17	2.55	2.12	0.998	0.109	0.103	0.109	25.92
PUR + A200 1%	7	2.34	15.35	0.999	0.213	0.196	0.213	28.30
PUR + A200 2%	7	2.49	9.23	0.999	0.187	0.176	0.187	28.99
PUR + A200 4%	7	2.49	7.45	0.999	0.172	0.162	0.172	24.33
	12	2.58	3.23	0.999	0.131	0.125	0.131	23.80
	17	2.46	1.35	0.999	0.084	0.079	0.084	23.91
PUR + A805 0.5%	7	2.31	16.96	0.999	0.219	0.201	0.219	25.28
	12	2.66	4.80	0.999	0.160	0.154	0.160	24.94
	17	2.69	1.10	0.997	0.095	0.091	0.095	25.42
PUR + A805 1%	7	2.03	32.07	0.993	0.257	0.220	0.257	28.73
PUR + A805 2%	7	2.24	16.41	0.989	0.208	0.188	0.208	28.58
PUR + A805 4%	7	2.50	8.91	0.999	0.186	0.175	0.186	24.27
	12	2.57	4.42	0.997	0.147	0.140	0.147	23.56
	17	2.58	1.37	0.996	0.094	0.090	0.094	23.90
PUR + A711 0.5%	7	2.47	10.02	0.998	0.191	0.180	0.191	24.67
	12	2.39	6.79	0.999	0.155	0.144	0.155	23.89
	17	2.59	1.26	0.999	0.092	0.088	0.092	25.91
PUR + A711 1%	7	2.31	13.84	0.999	0.200	0.184	0.200	29.45
PUR + A711 2%	7	2.48	10.73	0.999	0.198	0.186	0.198	28.91
PUR + A711 4%	7	2.58	6.87	0.999	0.175	0.167	0.175	24.57
	12	2.59	4.76	0.999	0.153	0.146	0.153	23.61
	17	2.52	1.57	0.998	0.094	0.089	0.094	23.87

n and k, Avrami kinetic parameters; R^2, coefficient of linear regression of fitting experimental data with Avrami model; K, $t_{1/2}$, and t_{max}, calculated according eqs. (4–6) respectively; ΔH_c, enthalpy of isothermal crystallization.

crystallization process in nanocomposites is faster than in neat PUR in the investigated range of silicas fractions up to 4 vol %. This can be assigned to the increase of the nucleation rate, which implies an increase in the number of nuclei per unit volume of PUR matrix, and a subsequent reduction in spherulite size distribution, what is in line with observations from polarizing micrographs.[19] Namely, substantial decrease in spherulite size up to fine spherulitic or even grain morphology with incorporation of all silica fillers have been observed.

Further, the obtained results presented in Figure 4 imply that at a relatively low content up to 1 vol % all silica fillers act as heterogeneous nuclei and accelerate crystallization. Further addition of the silica above this amount decreases crystallization rate. Similar results were obtained for the influence of silica filler on nonisothermal and isothermal crystallization of polyvinylalcohol[20,24] and nonisothermal crystallization of polypropylene.[25] Generally, possible explanations for decrease of the crystallization rate in systems with higher silica content are that the crystal growth may be retarded by confined interparticle distance at higher silica contents[20] or that the SiO_2 clusters act as barrier to retard the crystallization by depressing the crystal growth because of the interaction between SiO_2 clusters and matrix.[24] In our previous investigation of PUR/SiO_2 systems, we have found considerable decreasing of spherulite size by increasing fraction of all silica fillers that was assigned to confined interparticle distance.[19] In addition, previous investigations showed that at PUR/unmodified silica interface specific hydrogen interactions between silanol groups at silica surface and ester carbonyl groups in soft segments are established,[12–14] which can retard crystallization. Considering that all silica fillers, regardless of surface modification at higher content decrease crystallization rate, this is attributed to the confined interparticle distance. In contrast to the findings about influence of filler fraction in this work, hydrophobic fumed silica modified with dimethyldichlorosilane increases the value of constant K of polypropylene up to 10% by weight.[26]

The results also indicate that the octylsilane treated silica filler (A805) has a major impact on the rate of crystallization,

Applied Polymer SCIENCE

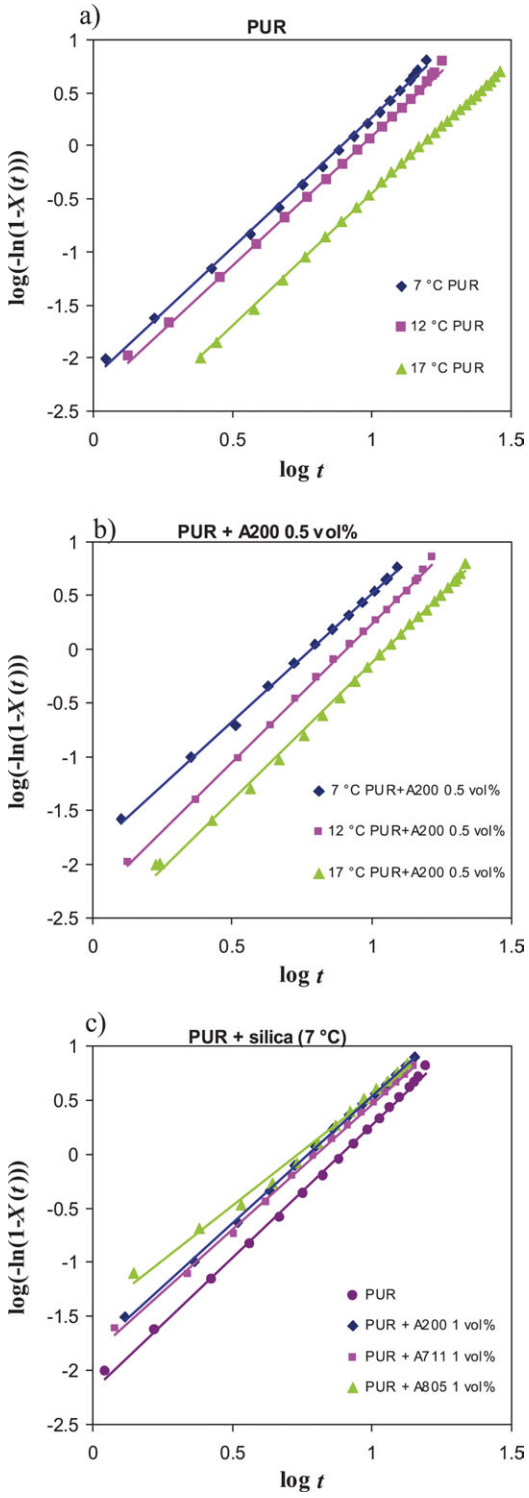

Figure 3. Avrami plots according eq. (3) for samples (a) neat PUR at different T_c (b) PUR + A200 0.5 vol % at different T_c and (c) PUR + different types of silica fillers at $T_c = 7°C$. [Color figure can be viewed in the online issue, which is available at wileyonlinelibrary.com.]

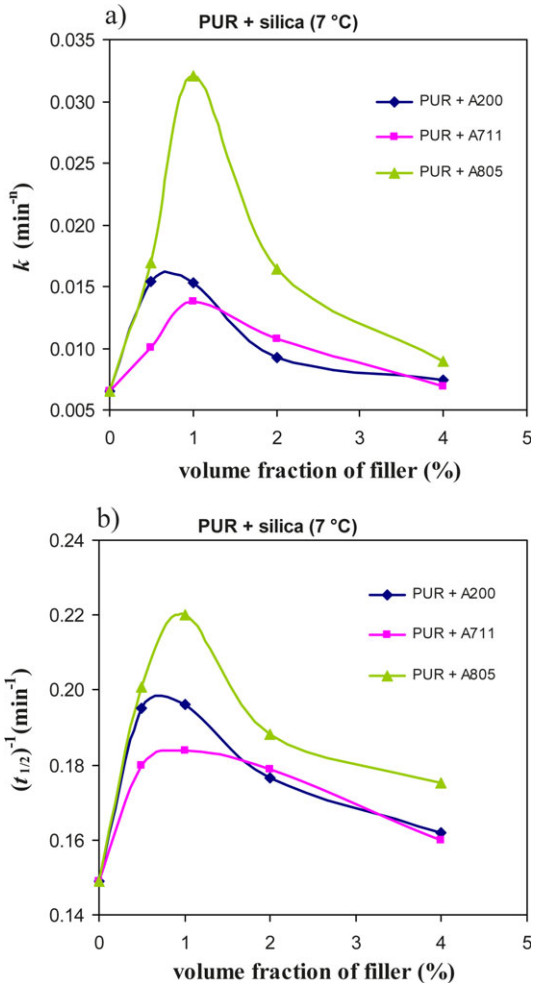

Figure 4. Influence of surface modification and amount of silica according to (a) Avrami crystallization rate constant k and (b) reciprocal value of half crystallization time $t_{1/2}$ calculated according eq. (4). [Color figure can be viewed in the online issue, which is available at wileyonlinelibrary.com.]

stronger than the unmodified filler (A200), while the filler modified with methacrylsilane (A711) has the smallest effect. The results of previous investigations[19] of these systems have shown that the filler modified with octylsilane due to the presence of alkaline chains at the surface has nonpolar character. As stated earlier, the crystallization in the study corresponds to the crystallization of PUR soft nonpolar segment. Previous investigations showed that modification of silica with octylsilane that form thick organic layer around particles ensure good redispersibility in acrylic polyol resin and consequently in acrylic based PURs.[35] Better dispersion of hydrophobic than hydrophilic silica was also observed in other PURs.[36] Nonpolar character of silica filler treated with octylsilane (A805) and consequently better distribution is the probable reason of the most pronounced influence of this filler on the crystallization of nonpolar soft segment of PUR matrix. Further, results indicate that up to 1 vol % of filler nanocomposites with nonmodified A200 silica filler have higher crystallization rate than nanocomposites with methacrylsilane A711 modified filler, thus indicating higher nucleation activity of nonmodified silica. Previous investigations showed that at PUR/silica interface specific hydrogen interactions are established and consequently result in better phase separation in systems with silica filler.[12–14] Based on these findings, we can presume that the higher crystallization rate of the

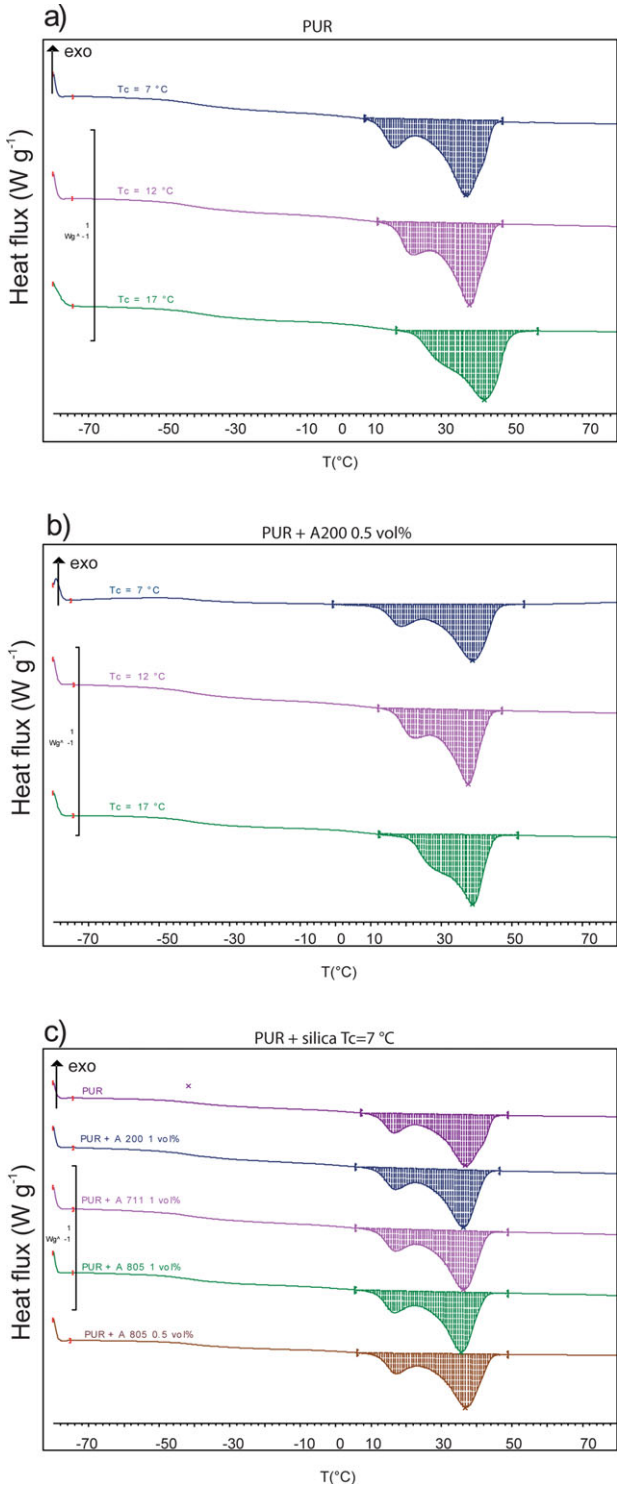

Figure 5. The DSC thermograms obtained during subsequent heating of isothermally crystallized samples (a) neat PUR crystallized at different T_c, (b) PUR + A200 0.5 vol % crystallized at different T_c, and (c) PUR + different types of silica fillers crystallized at $T_c = 7°C$. [Color figure can be viewed in the online issue, which is available at wileyonlinelibrary.com.]

nonmodified A200 filler in comparison to methacrylate modified filler can be assigned to the described specific interactions. The best mechanical properties of PUR nanocomposites with A200 in comparison to systems with A805 and A711 are also assigned to the specific hydrogen interactions between silica and PUR matrix.[19] Despite of the fact that polar unmodified (A200) and nonpolar silica filler modified with octylsilane (A805) exhibit similar effect on the crystallization rate of PUR soft segment, reason is different. Nonpolar octylsilane modified filler is uniformly distributed in nonpolar PUR phase and therefore increase crystallization rate, while polar silica filler establish interactions that favors phase separation between hard and soft phase and increase crystallization rate.

Melting of Isothermally Crystallized PUR/SiO_2 Nanocomposites

Figure 5 shows the melting curves of samples isothermally crystallized at different temperatures for PUR matrix [Figure 5(a)] and PUR nanocomposites with 0.5 vol % nonmodified filler A200 [Figure 5(b)]. From the presented curves, it is obvious that isothermally crystallized samples have significantly different melting behavior than PUR sample tested under nonisothermal DSC measurement (presented in our previous article[19]). Namely, at nonisothermal DSC thermogram in second heating cycle the cold crystallization and single melting peaks were visible.[17] Absence of the cold crystallization peak in heating curve of the isothermally crystallized samples at different temperatures [Figure 5(a,b)] confirm that at all crystallization temperatures samples reach their maximum crystallinity, and therefore during subsequent heating only melting peak appears. Further, presented melting curves of isothermally crystallized samples indicate multimelting behavior that significantly changes depending on temperature of isothermal crystallization for both neat PUR [Figure 5(a)] and PUR + A200 0.5 vol % nanocomposites [Figure 5(b)]. On presented curves, two endothermic peaks are visible, Peak I at lower temperature, Peak II at higher temperature and on the curves of some samples shoulder III at even higher temperature is visible. The values of temperatures and enthalpies of all investigated samples are presented in Table III. Results show that as the temperature of isothermal crystallization T_c increases from 7 to 17°C the Peak I shifts to higher temperatures from ~ 17 to 26.5°C and the enthalpy increases from 6–7 J/g to 10.8–12.8 J/g. The type of silica has no influence on the values of T_m(I) and ΔH_m(I). The enthalpy of melting Peak II decreases as T_c increases and temperature of peak increase only slightly for maximally 2°C. In general, the multiple melting behavior is observed for other isothermally crystallized polymers and composites.[29,31,37–40] The Peak I can be assigned to melting and simultaneous recrystallization of phase that crystallized during isothermal crystallization. Since at higher T_c temperatures more perfect crystallites form, the Peak I shifts toward higher temperatures. The Peak II is attributed to the melting of PUR matrix that results from processes of recrystallization and melting under Peak I and therefore is very slightly dependant on T_c. The fact that enthalpy of isothermal crystallization and enthalpy of melting differs significantly as presented in Figure 6 confirms that during the melting simultaneous processes of recrystallization occurs.

The melting curves presented in Figure 5(c) and data in Table III show that the temperatures of the endothermal melting Peaks T_m(I) and T_m(II) does not change significantly by

Table III. Values for Melting of Isothermally Crystallized Samples

PUR nanocomposites	T_c (°C)	ΔH_{tot} (J/g PUR)	ΔH_m(I) (J/g PUR)	T_m(I) (°C)	ΔH_m(II) (J/g PUR)	T_m (II) (°C)
PUR	7	32.10	6.29	16.58	25.81	36.83
	12	32.34	7.40	21.90	24.94	37.81
	17	30.20	10.84	28.58	19.36	42.01
PUR + A200 0.5%	7	32.37	6.68	16.91	25.70	36.22
	12	31.83	7.67	22.56	24.16	36.64
	17	28.97	11.92	26.73	17.06	38.98
PUR + A200 1%	7	34.03	7.43	16.91	26.60	36.15
PUR + A200 2%	7	34.83	7.48	16.90	27.35	36.14
PUR + A200 4%	7	31.46	6.63	17.08	24,87	36.33
	12	31.08	7.41	22.24	23.68	36.99
	17	30.14	11.58	26.23	18.57	39.16
PUR + A805 0.5%	7	32.55	6.93	17.24	25.62	36.82
	12	29.29	7.24	22.27	22.05	37.36
	17	31.03	12.49	26.56	18.09	38.65
PUR + A805 1%	7	34.44	7.41	16.74	27.03	36.00
PUR + A805 2%	7	34.60	7.52	17.07	27.08	35.97
PUR + A805 4%	7	31048	6.69	17.09	24.79	36.51
	12	31.24	7.30	22.87	23.94	37.45
	17	29.49	12.18	26.57	17.31	38.33
PUR + A711 0.5%	7	31.80	6.68	16.91	25.12	36.66
	12	30.05	7.30	22.76	22.74	37.67
	17	30.41	11.93	26.38	18.45	38.30
PUR + A711 1%	7	35.22	7.57	17.07	27.65	36.31
PUR + A711 2%	7	34.64	7.50	17.24	27.14	36.31
PUR + A711 4%	7	31.51	6.63	17.08	24.87	36.66
	12	31.27	7.62	22.41	23.64	37.16
	17	30.05	11.85	26.41	18.20	38.50

ΔH_{tot} total enthalpy, ΔH_m(I), and ΔH_m(II) enthalpies under melting Peaks I and II; T_m(I) and T_m(II) temperatures of melting for Peaks I and II.

increasing filler volume fraction or filler surface treatment (Table III). These results indicate that the addition of fillers does not change the structure of the crystallites. However, thermograms in Figure 5(c) show that addition of all fillers causes narrowing of the melting peaks, thus indicating that due to the presence of the filler the crystallite size distribution becomes narrower. Relative invariance of T_m(I) for nanocomposites at a certain T_c could be consequence of the equilibrium lamellar thickness reached the during isothermal crystallization which is difficult to prove since Peak I is due to simultaneous processes of melting and recrystallization.

In Figure 6, enthalpies of crystallization and melting at T_c =7°C versus mass fraction of filler phase for all investigated samples are presented. The values of enthalpies (Tables II and III; Figure 6) are normalized by the amount of PUR matrix in the system. Despite the fact that enthalpies of crystallization and melting differs significantly due to the recrystallization during the melting, both of them change similarly depending on the fraction of filler regardless of the silica surface modification. The addition of small amounts (0.5 vol %) of any filler does not change total

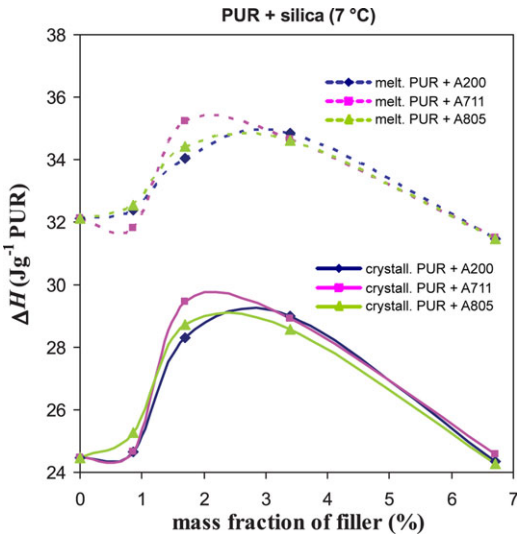

Figure 6. Influence of surface modification and amount of silica on the (a) enthalpy of isothermal crystallization ΔH_c and (b) melting enthalpy of isothermally crystallized samples ΔH_m. [Color figure can be viewed in the online issue, which is available at wileyonlinelibrary.com.]

enthalpy of melting. Further increase of the filler amount (1 and 2 vol %) increases degree of crystallinity, but the addition of 4 vol % of all the filler significantly reduces the enthalpies. It can be concluded that the addition of larger amounts of fillers causes the reduction of the crystallinity.

CONCLUSIONS

The influence of surface modification and amount of the fumed silica on the isothermal crystallization kinetic and melting of PUR soft segment were investigated. Crystallization kinetic of PUR and PUR nanocomposites can be properly described by Avrami's model. The obtained Avrami number n indicates that all samples, regardless the temperature of isothermal crystallization, amount of filler or filler surface modification, crystallize in the spherulitic three-dimensional manner.

As the temperature of isothermal crystallization increases crystallization rate decreases for all samples. However, crystallites formed at the higher crystallization temperature consequently melt at higher temperatures, thus indicating, that by increasing T_c more orderly crystallites are formed.

The kinetic rate constant k and $(t_{1/2})^{-1}$ indicate that nonmodified as well as modified silica fillers act as nucleating agent. The nucleating efficiency is the most pronounced in nanocomposites with 1 vol % of the filler. The filler modified with octylsilane has the strongest nucleation effect and the strongest effect on the crystallization rate what is attributed to the nonpolar nature of this filler and its preferable location and good distribution in nonpolar crystallizing soft phase of the PUR matrix. Results show better nucleation efficiency of the nonmodified silica, despite its high polarity, compared to the filler modified with methacrylsilane. This result can be explained with specific hydrogen interactions between silanol groups at silica surface and ester carbonyl groups in the PUR soft segments and consequently better phase separation and higher crystallization rate in systems with nonmodified silica filler.

The temperatures of the melting peaks T_m(I) and T_m(II) do not change significantly by increasing the amount of filler or changing the filler surface treatment what indicate that in all nanocomposites the perfection of the crystallites is similar regardless of the type or amount of filler. However, the enthalpies of crystallization and melting indicate that all silica filler in amounts of 1 and 2 vol % enhance crystallization of PUR soft segment.

ACKNOWLEDGMENTS

The authors thank to Dr. Domagoj Vrsaljko for help in preparing the figures. This research has been done within the national scientific project "Surface and interface engineering of nanoparticles in adhesive nanomaterials" funded by Ministry of science, education and sport of Republic of Croatia.

REFERENCES

1. Petrović, Z. S. Ferguson, J. *Prog. Polym. Sci.* **1991**, *16*, 695.
2. Krol, P. *Prog. Mater. Sci.* **2007**, *52*, 915.
3. Prisacariu, C.; Scortanu, E.; Airinei, A.; Bogdan Agapie, B.; Iurzhenko, M.; Mamunya, Y. P. *Procedia Eng.* **2011**, *10*, 446.
4. Buckley, C. P.; Prisacariu, C.; Martin, C. *Polymer* **2010**, *51*, 3213.
5. Janik, H.; Palys, B.; Petrovic, Z. S. *Macromol. Rapid Commun.* **2003**, *24*, 265.
6. Whitmore, M. D.; Noolandi, J. *Macromolecules* **1988**, *21*, 1482.
7. DiMarzio, E. A.; Guttman, C. M.; Hoffman, J. D. *Macromolecules* **1980**, *13*, 1194.
8. Zhou, S.; Wu, L.; Sun, J.; Shen, W. *Prog. Org. Coat.* **2002**, *45*, 33.
9. Chen, Y.; Zhou, S.; Yang, H.; Wu, L. *J. Appl. Polym. Sci.* **2005**, *95*, 1032.
10. Petrović, Z. S.; Javni, I.; Waddon, A.; Banhegyi, G. *J. Appl. Polym. Sci.* **2000**, *76*, 133.
11. Wypych, G. Handbook of fillers, 2nd ed.; ChemTec Publishing: Toronto, New York, **2000**; Chapter 2, pp 132.
12. Nunes, R. C. R.; Foneseca, J. L. C.; Pereira, M. R. *Polym. Test.* **2000**, *19*, 93.
13. Nunes, R. C. R.; Pereira, R. A.; Foneseca, J. L. C.; Pereira, M. R. *Polym. Test.* **2001**, *20*, 707.
14. Bistričić, L.; Baranović, G.; Leskovac, M.; Govorčin Bajsić, E. *Eur. Polym. J.* **2010**, *46*, 1975.
15. Vega-Baudrit, J.; Navarro-Banon, V.; Vazquez, P.; Martin-Martinez, J. M. *Int. J. Adhes. Adhes.* **2006**, *26*, 378.
16. Vega-Baudrit, J.; Sibaja-Ballestero, S.; Vazquez, P.; Terregrosa-Marcia, R.; Martin-Martinez, J. M. *Int. J. Adhes. Adhes.* **2007**, *27*, 469.
17. Navarro-Banon, V.; Vega-Baudrit, J.; Vazquez, P.; Martin-Martinez, J. M. *Macromol. Symp.* **2005**, *221*, 1.
18. Zhou, S. X.; Wu, L. M; Sun, J.; Shen, W. D. *J. Appl. Polym. Sci.* **2003**, *88*, 189.
19. Lučić Blagojević, S.; Buhin, Z.; Pustak, A.; Lukić Kovačić, R. *J. Appl. Polym. Sci.* **2012**, *125*, E181.
20. Lee, J.; Lee, K. J.; Jang, J. *Polym. Test.* **2008**, *27*, 360.
21. Ke, Y. C.; Wu, T. B.; Xia, Y. F. *Polymer* **2007**, *48*, 3324.
22. Estves, A. C. C.; Barros-Timmons A. M.; Martins, J. A.; Zhang, W.; Cruiz-Pinto, J.; Trindade, T. *Compos. B* **2005**, *36*, 51.
23. Kim, S. H.; Ahn, S. H.; Hirai, T. *Polymer* **2003**, *44*, 5625.
24. Peng, Z.; Kong L. X.; Li, S. D. *Polymer* **2005**, *46*, 1949.
25. Jain, S.; Goossens, H.; van Diun, M.; Lemstra, P. *Polymer* **2005**, *46*, 8805.
26. Papageorgiou, G. Z.; Achilias, D. S.; Bikiaris, D. N., Karayannidis, G. P. *Thermochim. Acta.* **2005**, *427*, 117.
27. Avrami, M. *J. Chem. Phys.* **1939**, *7*, 1103.
28. Avrami, M. *J. Chem. Phys.* **1940**, *8*, 212.

29. Chen, X.; Li, C.; Shao, W. *Eur. Polym. J.* **2007**, *43*, 3177.
30. Albano, C.; Papa, J.; Ichazo, M.; Gonzales, J.; Ustariz, C. *Comp. Struct.* **2003**, *62*, 291.
31. Naffakh, M.; Martin, Z.; Gomez, M. A.; Jamenez, I. *Thermochim. Acta.* **2008**, *472*, 11.
32. Cai, J.; Yu, Q.; Han, Y.; Zhang, X.; Jiang, L. *Eur. Polym. J.* **2007**, *43*, 2866.
33. Supaphol, P. *Thermochim. Acta.* **2001**, *370*, 37.
34. Dangseeyun, N.; Srimoaon, P.; Supaphol, P.; Nithitanakul, M. *Thermochim. Acta.* **2004**, *409*, 63.
35. Chen, G.; Zhou, S.; Gu. G.; Yang, H.; Wu, L. *J. Colloid. Interface Sci.* **2005**, *281*, 339.
36. Jalili M. M.; Moradian, S. *Prog. Org. Coat.* **2009**, *66*, 359.
37. Chen, M.; Chang W.-C.; Lu, H. Y.; Chen, C. H. Peng, J.-S.; Tsai, C.-J. *Polymer* **2007**, *48*, 5408.
38. Yasuniwa, M.; Iura, K.; Dan, Y. *Polymer* **2007**, *48*, 5398.
39. Supaphol, P.; Apiwanthanakorn, N.; Krutphun, P. *Polym. Test.* **2007**, *26*, 985.
40. Gunaratne, L. M. W .K.; Shanks, R. A. *Eur. Polym. J.* **2005**, *41*, 2980.